

Background Free Measurement of the Spectra of Low Energy Electrons Emitted as a Result of Auger Transitions in Metals

S.F. Mukherjee, K. Shastry, A.H. Weiss

Department of Physics, University of Texas at Arlington, Arlington, TX, USA, 76019

Positron annihilation induced Auger electron spectroscopy was used to obtain Cu and Au Auger spectra that are free of primary beam induced background by impinging the positrons at energy below the secondary electron emission threshold. The removal of the core electron via annihilation in the PAES process resulted in the elimination of post-collision affects. The spectrum indicates that there is an intense low energy tail (LET) associated with the Auger peak that extends all the way to 0 eV. The LET has been interpreted as being due to processes in which the filling of the core by a valence electron results in the ejection of two or more valence electrons which share the energy of the otherwise Auger electron

PACS numbers: 78.70.Bj, 82.80.Pv, 68.49.-h, 79.20.Hx, 79.60.Bm

I. INTRODUCTION

Electron and X-ray induced Auger electron spectroscopy (EAES and XAES) are extremely sensitive to the composition and chemistry of the surface¹⁻³ owing to the short inelastic mean free path of electrons (5Å – 20Å) emitted in the Auger energy range ($\sim 20-2000$ eV)^{4,5}. Both these techniques use an incident beam energy greater than the ionization energy of the core electron (E_C) that is removed in order to initiate the Auger process. The energy of the emitted electron as a result of filling up of the initial hole is less than E_C due to the energy associated with the two hole final state of the Auger process. Consequently, the Auger peaks in EAES and XAES are superimposed upon a background composed of an electron cascade⁶⁻⁸ caused by the inelastic scattering of the incident electron beam or photo excited valence electrons. Such background tend to be many times the intensity of the Auger peak itself. In both the cases of EAES and XAES the background is considered extrinsic to the Auger process and is typically subtracted⁹⁻¹¹ to reveal the true Auger spectrum.

In this paper, we present full range spectrum of the electrons emitted following the creation of core hole using positron annihilation induced Auger electron spectroscopy (PAES) (as shown in Fig. 1a). Recently, it has been shown that it is possible to efficiently trap positrons directly in a surface state and excite Auger electrons by using a low positron beam energy (~ 1.5 eV) which is well below the threshold for secondary electron emission¹². Here, we have used this effect to measure the first completely background free Auger spectrum down to 0 eV. The surface state trapped positrons tunnel into the core region and annihilate with the electrons leading to the Auger process. The localization of the positrons in the surface state ensures that almost all of the excitations that result in Auger transition occur in the topmost atomic layer¹³. This is in contrast to conventional Auger spectroscopy (XAES or EAES) where, due to the penetrating nature of the incident beam, Auger electrons are excited at depths far in excess of the electron inelastic

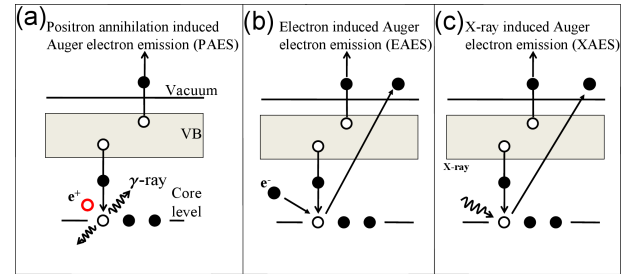


FIG. 1. (Color online) Energy band diagram showing mechanism for (a) PAES (b) EAES and (c) XAES. In PAES, the core hole is created by matter-antimatter annihilation and hence it is possible to get Auger emission with incident positron energy $E_p \rightarrow 0$ eV. As opposed to EAES and XAES, the post collision interaction (PCI) effects are absent in PAES since the core electron is annihilated.

mean free path. Such spectra are further complicated by post collision interaction (PCI) effect which refers to the interaction of the excited system (solid with a core hole) with the excited core electron. Such effect leads to plasmon loss features in X-ray photoelectron spectra and a consequent plasmon gain feature in the Auger spectra. This effect is absent in PAES as the Auger process is initiated by annihilation of the core electron. The low energy signals from conventional AES also contain the beam induced background which is typically many times more intense than the signal due to the Auger process. In clear contrast, a 1.5 eV positron induced PAES spectrum contains contributions that result directly or indirectly from Auger transitions in the top-most atomic layer.

Based on these considerations, PAES spectra can be understood and analyzed based on just two factors- the usual Auger peak (C-VV transition) and the intrinsic loss (C-VVV transition)¹ [C=Core, V=Valence]. The intrinsic loss associated with creation of a core hole has mostly been studied in context of the asymmetry in the photopeak and presence of intrinsic plasmons in X-ray photoelectron spectroscopy (XPS) and is referred to

as Mahan-Nozieres-DeDominicis effect^{4,14–17}. The intrinsic loss reflects as a tail on the low energy side of the core peak and is assumed to extend to $\sim 50\text{eV}$ below the peak⁴. The distinction between intrinsic and extrinsic electrons is based on the observation that the latter were related to electron transport in the solid while the former were due to creation of the core hole. Since the creation of core hole and the associated Auger process are essentially a single step process¹⁸ similar asymmetries should be present in Auger peaks as well. Experimental verification of this has been attempted solely by Auger-photoelectron coincidence spectroscopy (APECS) where a clear distinction between extrinsic and intrinsic electrons cannot be made^{19–21}. Hence an exact quantitative and qualitative prediction over the whole energy range has been missing. In PAES the core hole creation probability is independent of the incident positron energy which allows us to set the incident positron energy ($E_p = 1.5\text{ eV}$) well below the secondary electron creation threshold. The resultant spectra show a low energy tail (LET)¹⁹ with intensity (I_{LET}) $\sim 3.92(3.43)$ times that of the Auger peak intensity (I_{Auger}) for Cu(Au) at energies below the Auger energy and extending to 0 eV. The LET has been interpreted as arising mostly from intrinsic loss associated with the creation of the core hole. The spectral weight of intrinsic part of the LET is $2.39(3.0)$ times that of the Auger peak area which has been concluded as evidence of multi electron emission once the core hole is created. This process is analogous to the double Auger process in noble gases²² and similar to photon induced correlated electron emission from solids²³. The results have been interpreted as signature of electron correlation in the valence band^{19,21}.

II. EXPERIMENTAL

The experiments were carried out in the time of flight -positron annihilation induced Auger electron spectrometer (tof-PAES)²⁴ which uses a magnetic bottle analyzer²⁵. Positrons emitted via beta decay from a 4 mCi $Na-22$ source were moderated using a polycrystalline Tungsten (W). The upper limit on the positron beam energy, E_P , is given by the following equation

$$E_p = \varphi_m^+ + e(V_m - V_s) \quad (1)$$

where φ_m^+ is the positron work function of the moderator (2.9 eV for W), V_m and V_s are the bias on the moderator and sample with respect to the ground and e is the electronic charge. The low energy positrons are guided to the sample, located 3.5 m away, using EXB fields. The whole spectrometer is housed in Helmholtz cage to cancel out the earth's magnetic field. The energy of the outgoing electron is referred to the vacuum level.

The annihilation gamma rays are detected by BaF_2 and NaI detectors as shown in Fig. 2a. The outgoing electrons from the sample are parallelized using the divergent field of a permanent magnet. The electrons then

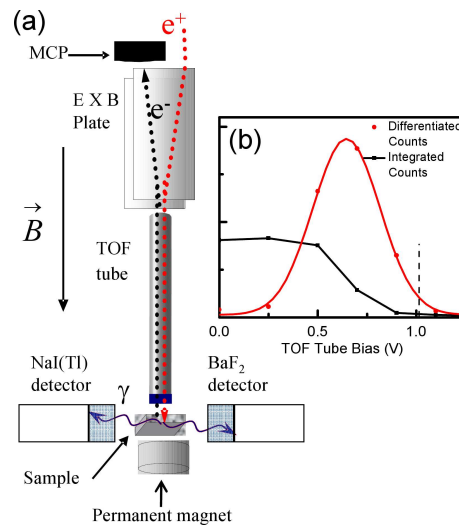


FIG. 2. (Color online) Experimental setup for time of flight-positron annihilation induced Auger electron spectroscopy (tof-PAES)(a) Schematic of the spectrometer.(b)The incident positron beam energy used to obtain the Auger spectra. The dashed line(1 eV) refers to the incident positron energy and 99%of positrons have energy less than this value (e^+ =positrons, e^- =electrons, B= magnetic field)

fly down a retarding time of flight tube (tof tube) and are detected by a Micro channel plate (MCP). The MCP signal is used as the START while the delayed BaF_2 signal provides the STOP (reverse timing) of the Time to Amplitude convertor (TAC). The TOF-PAES spectra are obtained by histogramming the output of the TAC. A calibration procedures detailed in reference¹² was used to determine the relation between the measured time of flight and the kinetic energy of the electrons leaving the sample. To estimate the contribution of accidental coincidence to tof-PAES spectra, a second setup referred to as the triple coincidence setup was used which takes advantage of the fact the annihilating gamma rays are emitted at an angle of $\sim 180^\circ$ with respect to each other. In this the STOP signal is the coincidence detection of the collinear 511 keV gamma rays by BaF_2 and NaI(Tl). The triple coincidence set up, by requiring the detection of two almost antiparallel gamma rays, was designed to discriminate against events in which one or both of the annihilation gamma rays generate secondary electrons as a result of Compton scattering in the sample or surrounding chamber walls.

The 4 mT transport field used in the TOF spectrometer is particularly well suited for efficiently transporting the low energy positron (which was incident at 1.5 eV at the sample) as well as the low energy electrons emitted from the sample. A -0.5 volt sample bias was used to boost the kinetic energy of electrons emitted from the surface permitting measurements of electrons emitted from the surface all the way down to 0 eV. The time of flight for a 0.5 eV electron (corresponding to 0 eV KE

emission from the sample) was $\sim 2\mu\text{s}$ which was well within the measuring range of the spectrometer.

The incident beam profile (shown in Fig. 2(b)) at 0 eV sample bias was fitted with a Gaussian of 0.4 eV FWHM and maximum at 0.65 eV. 99 % of the positrons have energy less than 1 eV and this is referred to as the beam energy. This beam energy was used to obtain the Auger spectra of Cu and Au. During the measurements of the Auger spectra, the sample was biased at -0.5 V with respect to the TOF drift tube.

An Au sample (a 99.985 % pure polycrystalline foil, 0.025 mm thickness) was sputter cleaned every 12 hours while a Cu(100) sample (a 99.9 % pure, 10 mm diameter \times 1 mm thickness) was sputter cleaned followed by annealing at 740 $^{\circ}\text{C}$ every 12 hours. The PAES spectrum was used to monitor the cleanliness of the sample and no significant contamination of the surface was found in the period between two sputtering times.

The sensitivity of PAES to the low energy electrons (≥ 0.5 eV) is demonstrated in spectra shown in Fig. 3 which were obtained with an incident beam energy of 2 eV. The incident positron energy was changed by varying the moderator bias (Eq 1) while keeping the electric and magnetic fields between the sample and MCP same. The peaks in the timing spectra (Fig. 3) are the Auger peak and the positron sticking induced secondary electron peak¹². The lagging edge of the secondary electron peak (corresponding to the longest flight times) moves to shorter flight time as the sample bias is increased from -0.5 V to -1 V. These results confirm the ability of the tof-PAES system to detect and measure the energy of electrons emitted from the sample down to sub-eV energies. To obtain the Auger spectra, the moderator voltage was changed back to get a 1 eV beam incident on the sample at 0V bias. All the Auger spectra were taken with this setting and sample bias -0.5 V.

III. RESULT AND DISCUSSION

The PAES spectra from Cu and Au are shown in Fig. 4. The Auger peaks in the case of Cu and Au are $M_{23}VV$ and $O_{23}VV$ respectively. The LET can be seen to extend from 0–50 eV for Cu and 0–30 eV for Au. The argument that the LET is due to the Auger electrons only can be ruled out by noting that secondary electron yield (δ) will be $\sim 3.92(3.43)$ for Cu(Au) while the maximum value of δ for most metals is 1.8²⁶. Unlike earlier study of Cu $M_{2,3}VV$ Auger peaks²⁷, we did not observe any plasmon peaks on the low energy side of the Auger peak which is consistent with other PAES studies^{28,29}.

LET associated with the Auger peak has been earlier studied by Auger-photoelectron coincidence spectroscopy (APECS)^{19,20} and PAES²⁸. Both the studies were limited in the energy range studied (30 – 70 eV for APECS and 18 – 70 eV for PAES). The APECS spectra were further limited as the signal was an average over several atomic layer (~ 2) and a background due to true coin-

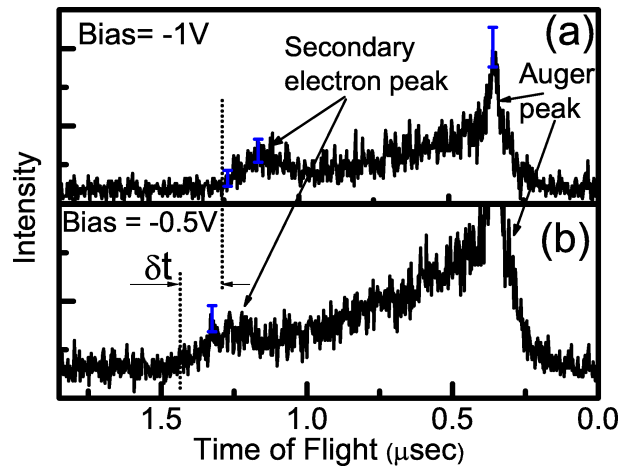


FIG. 3. PAES spectra from Au obtained with a bias of -1 V and -0.5 V. The spectra contains sticking induced secondary electron peak¹² and Auger peak. The incident positron beam energy at 0 V sample bias is 2 eV. The spectra is sitting on a flat background due to accidental coincidences. The vertical dotted line in both the panels shows the lagging edge of the secondary electron peak which corresponds to electrons leaving the sample with 0 kinetic energy just outside the surface. The lagging edge shifts to higher flight time as the negative bias is increased demonstrating that PAES is capable of detecting electrons with energy more than 0.5 eV.

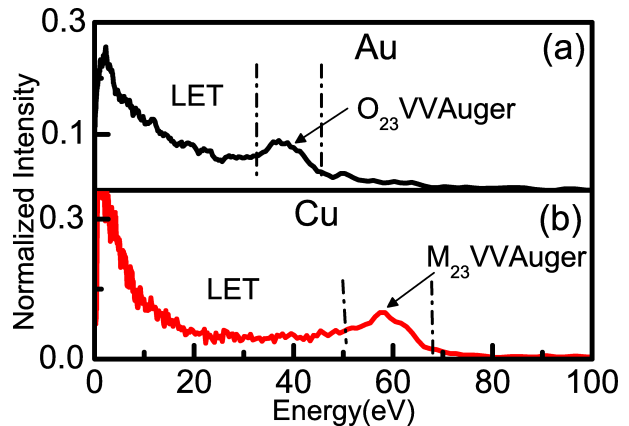


FIG. 4. (Color online) PAES spectra of (a) Au ($O_{23}VV$) and (b) Cu ($M_{23}VV$) obtained using a 1.5 eV positron beam and a -0.5 V bias on the sample. The energy scale represents the kinetic energy of the electrons leaving the surface of the sample. The region enclosed by dashed lines is due to the usual C-VV Auger transition while the intensity on the left side is the low energy tail.

cidences involving inelastically scattered photo electrons from the valence band. Earlier PAES experiments employed a positron beam of ~ 18 eV and hence the low energy part of such spectra were dominated by extrinsic electrons. In the experiments reported here, the Auger signal comes from the topmost layer of the atoms³⁰ and

the primary beam induced secondary electrons are energetically forbidden. Hence the PAES spectrum should contain the major spectral weight in the allowed Auger transition energy region, $E_C - 2V < E < E_C$, where E_C is binding energy of the core electron, V is the width of the valence band and E is the energy of the electron. In our experiments, we find that majority of the intensity is in LET region (Fig. 4).

Following the argument of Ref. 19 and 20, the LET intensity associated with the Auger peak can be broken down to intrinsic and extrinsic contributions

$$I_{LET}(E) = I_{LET}^{Intrinsic}(E) + I_{LET}^{Extrinsic}(E) \quad (2)$$

where $I_{LET}(E)$ is the spectrum in LET region and the factors on the right side of the equation are the intrinsic and extrinsic contributions to it. The extrinsic part, in a usual Auger spectrum, is caused by primary beam and the transport of the Auger electrons through the solid. As suggested in Ref. 7 and 8, the extrinsic part can be broken down into two components

$$I_{LET}^{Extrinsic}(E) = I_{beam}(E) + I_{Auger}^{Extrinsic}(E) \quad (3)$$

where $I_{beam}(E)$ is the primary beam induced secondary electron spectrum, $I_{Auger}^{Extrinsic}(E)$ is the spectrum due to the Auger electron scattering inelastically with surface and subsurface atoms⁷. The area under the Auger peak in PAES spectrum (50 – 70 eV for Cu and 30 – 50 eV for Au) is referred to as I_{Auger} . The inherent assumption in these analysis is that creation of Auger electrons and their subsequent emission can be treated separately³¹.

As discussed above, we used an incident beam whose energy was below the threshold energy that could cause secondary electron emission. It has been demonstrated in Ref. 12 that the threshold for positron induced secondary electron emission is given by:

$$E_{Kmax} = E_p - \varphi^- + E_b \quad (4)$$

where E_{Kmax} is the maximum energy of emitted electron, φ^- is the electron work function and E_b is the binding energy of the positron in the image potential well¹². For Cu(Au), $\varphi^- = 4.6(5)$ eV³² and $E_b = 2.7(2.9)$ eV and hence the threshold for secondary electron emission is 2 eV. The Auger spectra shown in Fig. 4 were obtained with an incident beam whose kinetic energy on the sample surface was 1.5 eV thus making the beam induced secondary electron emission channel energetically forbidden.

Earlier studies³³ have shown that backgrounds due to positron annihilation-gamma ray induced secondary electrons were not significant in the PAES measurements. These experiments showed that it was possible to turn off the positron annihilation induced Auger signal by thermally desorbing the positrons from the surface state into the vacuum as positronium Ps (a hydrogen like atom composed of an electron and positron). Most of the Ps annihilate in close proximity to the sample. Consequently if gamma ray induced secondary electrons were a

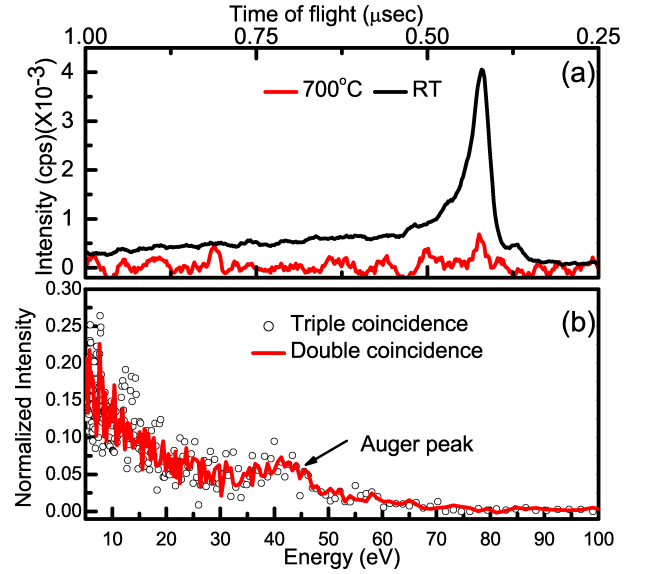


FIG. 5. (Color online) Estimation of gamma induced secondary electron contribution to LET (a) Comparison of PAES spectrum of Cu obtained at room temperature(RT) and at 700°C. (b) Normalized PAES and triple coincidence spectra from Au surface. The triple coincidence setup is biased against gamma ray induced background.

significant source of background signal, that signal should still be present even after the positrons are desorbed from the surface state as Ps. The data in Fig. 5(a) show the results of experiments, which are similar to Ref. 33. The average count of the high temperature spectrum(700°C) are only $\sim 2\%$ of the RT count rates (obtained after cooling the sample to room temperature). This provides an upper bound on the gamma induced secondary background of $\sim 2\%$ of the observed signal from the LET and demonstrates that gamma induced secondaries are not an important source of background in our measurements. The fact that the signal returned after the sample is cooled demonstrates that heating the sample did not produce significant contamination of the surface.

Further verification of the absence of this channel is done by comparing the PAES signal to the triple coincidence setup described above. In the latter, a measured coincidence between the two annihilation gamma rays, emitted at $\sim 180^\circ$ angle to each other, was required in order to produce a valid STOP signal to the TAC. The triple coincidence measurement insured that the annihilation events were taking place at the sample since two gamma annihilation taking place at some distance from the sample would not be in the simultaneous view of both detectors. The requirement of triple coincidence would strongly suppress background due to annihilation induced secondary electrons generated on surfaces other than the sample. The triple coincidence set-up will also strongly suppress events where one of the gamma rays undergoes Compton scattering or photo emission in the

sample. The PAES and the triple coincidence spectrum from Au are shown in Fig. 5(b). The LET region (0 – 30 eV) can be seen to have similar intensity in both the PAES and triple coincidence spectra (the poorer statistics of the triple coincidence measurements are a consequence of the low count rate associated with the reduced joint detection efficiency of the two gamma detectors) proving that the gamma induced background has negligible contribution in LET.

Next, the extrinsic contribution to the LET by the Auger electrons undergoing scattering in the surface and subsurface region is explored. The inset in Fig. 6(a) represents an isotropic source of Auger electrons in the top-most atomic layer⁷. The electron source is confined to the first atomic layer because of the high surface selective nature of PAES. The emitted electrons are divided amongst three types based on their probability of undergoing inelastic scattering. Region 1 corresponds to the Auger electrons that escape the solid without suffering any inelastic or elastic collision and are eventually detected. These electrons show up as the peak in the Auger spectrum. Not all the electrons emitted in the forward direction will fall in this category. The ratio of such electrons to all Auger electrons emitted in forward direction is referred to as transmission probability (T). Region 2 corresponds to those electrons which are emitted at a fairly large angle to the surface normal and hence will scatter inelastically with the selvedge layer. The ratio of such electrons to the total auger electrons in forward direction is given by $1 - T$. As discussed below, these electrons have shown to be contributing mostly to the cascade region (< 30 eV for Cu). Region 3 corresponds to the Auger electrons that are emitted towards the subsurface region and are assumed to be completely lost in the cascade process. Since isotropic nature of Auger emission is assumed, the number of electrons in region 3 will be the equal to the sum of those in region 1 and 2. The transmission factor, T, has been calculated using the Beer lamberts cosine law and is written as³⁴

$$T = \frac{\int_0^{2\pi} d\phi \int_0^{\pi/2} \exp\left(\frac{-d}{\lambda_{Cu,Au} \cos\theta}\right) \sin\theta d\theta}{\int_0^{2\pi} d\phi \int_0^{\pi/2} \sin\theta d\theta} \quad (5)$$

where $\lambda_{Cu,Au}$ is the inelastic mean free path of the Auger electron from Cu(Au)³⁵, d is the distance the electrons travel in the solid (1Å), θ is the angle from the surface normal and ϕ is the azimuthal angle. Hence, $T=50\%(59\%)$ has been calculated for Cu- $M_{23}VV$ (Au- $O_{23}VV$) Auger electron. The PAES spectra from Cu surface with different coverage of residual gases is shown in Fig. 6(b). It can be noticed that the major affect of altering the surface roughness or chemistry is in the low energy part of the LET (< 30 eV for Cu). This leads us to conclude that the Auger electrons from region 2 (Fig. 6(a)) contribute mostly to the cascade region of the LET. The secondary electron spectrum produced by inelastic scattering of the Auger electrons (represented by 2 and 3) has been modeled as suggested by Ref. 6

and is expressed as $I(E) \sim E(E + E_{PB})^{-1}(E + \Phi)^{-m}$, where $I(E)$ is the intensity of the secondary electron spectrum, E is the energy of the electron, E_{PB} is the energy of the primary beam, Φ is the work function of the metal and m is a constant. In our case, E_{PB} is taken as the Auger peak energy and is 60 eV for Cu- $M_{23}VV$ and 40 eV for Au- $O_{23}VV$ transition. This abovementioned line shape is for a beam energy of 30 and 300 eV normally incident on a polycrystalline copper surface while the electrons emitted from one specific angle is detected. This is in contrast to tof-PAES where the spectra are angle integrated. Hence, for the sake of comparison, we have measured the 60 eV positron induced secondary electron spectrum from Cu surface using tof-PAES (Fig. 6(a)). Here we have used the result that positron and electron induced secondary electron yields tend to be similar³⁶. It can be seen that the shape of the positron induced and theoretical secondary electron spectrum are quite similar providing extra confidence in modeling the Auger induced secondary electron spectrum by the form mentioned by Ref. 6. The area under the secondary electron curve (Fig.6(a)) has been normalized such as to yield a $\delta = 0.46(0.21)$ for Cu (Au) with a primary beam intensity of $I_{Auger}[(1 - T)/T + 1/T]$. Here, I_{Auger} refers to the area under the Auger peak (50 – 70 eV for Cu and 40 – 50 eV for Au) while the first term in the bracket refers to the electrons from the region 2 and the last term refers to electrons from region 3. Thus the spectral weight of the extrinsic part can be written as $\int_0^{E_0} I_{LET}^{Extrinsic} dE = \delta I_{Auger}[(1 - T)/T + 1/T]$, where E_0 represents the upper limit of LET (50(30) eV for Cu(Au)).

Representing the integrated terms by the respective intensity terms ($\int I(E)dE \rightarrow I$) and dividing both sides by the Auger peak area (I_{Auger}),

$$I_{LET}^{Intrinsic}/I_{Auger} = I_{LET}/I_{Auger} - \delta I_{Auger}[(1 - T)/T + 1/T] \quad (6)$$

Substituting the values Cu(Au) ($I_{LET}/I_{Auger} = 3.92(3.43)$, $\delta = 0.46(0.21)$ and $T = 0.51(0.59)$), the ratio of the intrinsic part of the LET to the Auger peak area ($I_{LET}^{Intrinsic}/I_{Auger}$) for Cu(Au) is 2.4(3.0).

The Cu- $M_{23}VV$ and Au- $O_{23}VV$ Auger transition with the estimated extrinsic contribution subtracted is shown in Fig. 7. The ratio of spectral weight in the main Auger peak to the intrinsic LET region is 1: 2.6(3.1). The intrinsic LET can be interpreted as due to the core holes decaying via multi electron emission process and is referred to as C-VVV process¹. The intrinsic emission is mostly thought of in terms of sudden limit which means that the core hole was created in a timeframe less than that of the Auger lifetime ($\sim fs$)⁴⁰. If the time taken to create the core hole is less than the Auger lifetime then the process is termed adiabatic³⁷. Adiabatic process is evident mostly in resonant emission as the outgoing photoelectron has small velocity so that the valence electrons, effectively, see no change in the effective charge. To establish the timescale in which the core hole is created in PAES, we

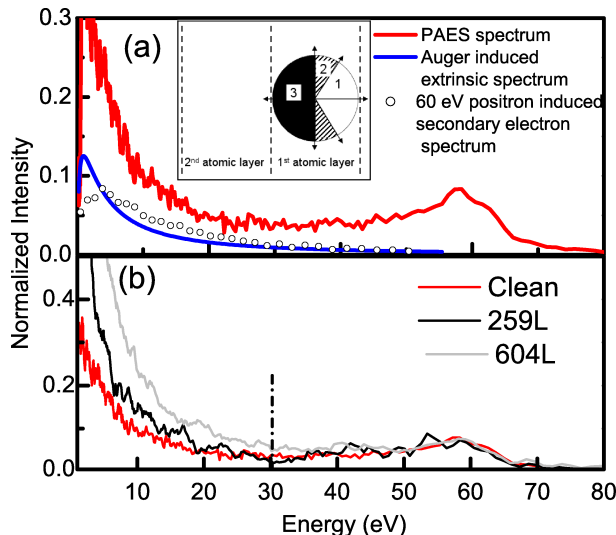


FIG. 6. (Color online) Estimate of the extrinsic background due to the Auger electrons scattering in the surface and subsurface region from Cu surface. (a) The normalized secondary electron spectrum as suggested by Ref 6 has been compared to the 60 eV positron induced secondary electron spectrum as recorded by TOF-PAES. The inset shows an isotropic Auger source located in the topmost atomic layer [Region 1 = the Auger electrons which are emitted without any inelastic scattering, Region 2 = Auger electrons which scatter inelastically from the surface, Region 3 = Auger electron scattering from the subsurface region⁷] (b) Normalized Cu-PAES spectra with different coverage of residual gas. As can be seen, the effect of surface scattering is mostly in the cascade region (< 30 eV).

have to consider the time taken by the positron to tunnel into the core region (~ 100 ps)^{38,39}. Hence the valence electrons see some effective charge, say Z , which changes slowly (~ 100 ps) from $Z + 1$ as the positron tunnels into the core region. This is followed by rapid annihilation ($\sim 10^{-23}$ sec)³⁹ while the effective charge seen by the valence electrons remains at $Z + 1$. Hence the PAES process can be considered to be in adiabatic regime and here we show that such emissions are possible in adiabatic regime as well.

The spectrum in Fig. 7 has been used to calculate the probability of core holes decaying via C-VVV process. Since such a process entails emission of two electrons (sharing the energy of the usual Auger electron), the spectral weight of the C-VVV process will be twice that of the conventional CVV process. Hence the percentage of core holes decaying via multi electron emission for Cu(Au) has been calculated to be $\sim 54(60)\%$. The C-VVV emission probability has also been used to calculate the positron-core electron annihilation probability at surfaces. Earlier calculations¹³ considered only the core-holes which decayed via the CVV process. Hence a 3.1% and 3% core annihilation probability was calculated for Cu(3p) and Au(5p). Based on our experiments,

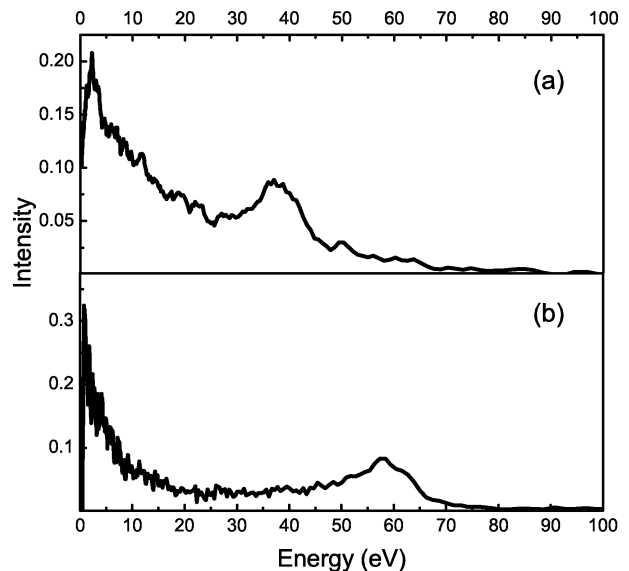


FIG. 7. (Color online) CVV Auger spectra of (a) Au and (b) Cu after the subtraction of extrinsic contribution. The intrinsic LET (C-VVV transition) extends to ~ 0 eV and is $\sim 2.4(3.0)$ times as intense as the Auger peak (C-VV transition) in case of Cu(Au).

we find the respective annihilation probability would be 6.8% and 7.5% which compares well with recent theoretical estimate^{41,42}.

IV. CONCLUSION

We have reported the first background free measurement of the complete spectra of low energy electrons emitted as a result of Auger transition in metals. By depositing low energy (~ 1.5 eV) positrons directly into the surface state¹² it was possible to excite Auger transitions from atoms at the surface without generating any primary beam induced secondary electrons. Localization of the positrons in the surface state ensures that almost all of Auger transitions occur in the topmost atomic layer. The resultant spectra showed that majority of the spectral weight is in the low energy tail associated with the Auger peak and extends to 0 eV. Estimates based upon measurements of the electron induced secondary electron yield and inelastic scattering probability of electrons with selfedge indicate that extrinsic contributions account for less than 36(14)% of the LET in case of Cu(Au). Our results suggest that the intrinsic part of LET is due to the process in which the core hole decays by emission of more than one Auger electron (C-VVV). Assuming that the intrinsic process involves emission of only two electrons, it has been calculated that 54(48)% of the core holes in Cu(Au) decay via multi electron emission. This result was used to obtain new estimate of positron-core electron annihilation probability for Cu and Au which

agree well with theoretical calculations. Since in the case of multi electron Auger emission, the valence electrons are emitted simultaneously, our studies are analogous to spectroscopy of photon induced emission of electron pairs²³ and provide another way of probing electron correlation effects in valence band of metals. Our results also have important implications in quantitative analysis of Auger spectra⁹. In particular, we show that a significant fraction of core holes decay via multiple electron processes. These processes result in a decrease in the Auger peak intensity that is not fully accounted for in the usual Beer-Lambert based calculations of the escape probability. Consequently, estimates based upon measur-

ing of the integrated intensity in the Auger peak region alone may lead to an underestimate of the number of initial core hole excitations. This has important implication for the use of PAES in estimating core hole annihilation probabilities⁴¹ and for the use of Auger spectroscopy in the quantitative analysis of surfaces.

V. ACKNOWLEDGEMENT

We wish to acknowledge useful discussion with D. E. Ramaker, J.Moxom and A.G.Hathaway. This work was supported by the Welch Foundation, Y1100 and NSF Grant No.DMR – 0907679.

- ¹ D. E. Ramaker, Journal of Vacuum Science & Technology A **7**, 1614 (1989).
- ² W. S. M. Werner, W. Smekal, H. Störi, H. Winter, G. Stefani, A. Ruocco, F. Offi, R. Gotter, A. Morgante, and F. Tommasini, Phys. Rev. Lett. **94**, 038302 (Jan 2005).
- ³ M. I. Trioni, S. Caravati, G. P. Brivio, L. Floreano, F. Bruno, and A. Morgante, Phys. Rev. Lett. **93**, 206802 (Nov 2004).
- ⁴ S. Tougaard, Surface and Interface Analysis **11**, 453 (1988).
- ⁵ M. Seah, Surface Science **32**, 703 (1972).
- ⁶ M. Seah, Surface Science **17**, 132 (1969).
- ⁷ E. N. Sickafus, Phys. Rev. B **16**, 1448 (Aug 1977).
- ⁸ E. N. Sickafus, Phys. Rev. B **16**, 1436 (Aug 1977).
- ⁹ M. Seah, Surface and Interface Analysis **24**, 830 (1996).
- ¹⁰ V. Contini, C. Presilla, and F. Sacchetti, Surface Science **210**, 520 (1989).
- ¹¹ D. Ramaker, J. Murday, and N. Turner, Journal of Electron Spectroscopy and Related Phenomena **17**, 45 (1979).
- ¹² S. Mukherjee, M. P. Nadesalingam, P. Guagliardo, A. D. Sergeant, B. Barbiellini, J. F. Williams, N. G. Fazileev, and A. H. Weiss, Phys. Rev. Lett. **104**, 247403 (June 2010).
- ¹³ K. O. Jensen and A. Weiss, Phys. Rev. B **41**, 3928 (March 1990).
- ¹⁴ G. D. Mahan, Phys. Rev. **163**, 612 (Nov 1967).
- ¹⁵ P. Nozières and C. T. De Dominicis, Phys. Rev. **178**, 1097 (Feb 1969).
- ¹⁶ S. Doniach and M. Sunjic, J. Phys. C: Solida State Phys. **3**, 285 (1970).
- ¹⁷ S. Hufner, "Photoelectron spectroscopy," (Springer, 1994) pp. 112–119.
- ¹⁸ E. Jensen, R. A. Bartynski, S. L. Hulbert, E. D. Johnson, and R. Garrett, Phys. Rev. Lett. **62**, 71 (Jan 1989).
- ¹⁹ E. Jensen, R. A. Bartynski, R. F. Garrett, S. L. Hulbert, E. D. Johnson, and C.-C. Kao, Phys. Rev. B **45**, 13636 (Jun 1992).
- ²⁰ C. P. Lund, S. M. Thurgate, and A. B. Wedding, Phys. Rev. B **49**, 11352 (Apr 1994).
- ²¹ G. v. Riessen, Z. Wei, R. S. Dhaka, C. Winkler, F. O. Schumann, and J. Kirschner, Journal of Physics: Condensed Matter **22**, 1 (Feb 2010).
- ²² T. A. Carlson and M. O. Krause, Phys. Rev. Lett. **14**, 390 (Mar 1965).
- ²³ N. F. Smith, J. D. Flannery, J. Henk, and P. Bruno, Phys. Rev. Lett. **89**, 086402 (Aug 2002).
- ²⁴ S. Xie, *Positron annihilation induced Auger electron spectroscopy of inner shell transitions using the time-of-flight technique*, Ph.D. thesis, University of Texas at Arlington (2002).
- ²⁵ P. Kruit and F. H. Read, Journal of Physics E: Scientific Instruments **16**, 313 (1983).
- ²⁶ Y. Lin and D. C. Joy, Surface and Interface Analysis **37**, 895 (2005).
- ²⁷ G. Chiarello, A. Amoddeo, R. G. Agostino, L. S. Caputi, and E. Colavita, Phys. Rev. B **48**, 7779 (Sep 1993).
- ²⁸ H. Zhou, *Auger Line Shape Measurements Using High Resolution Positron Annihilation Induced Auger Electron Spectroscopy*, Ph.D. thesis, University of Texas at Arlington (1996).
- ²⁹ C. Hugenschmidt, J. Mayer, and K. Schreckenbach, Journal of Physics: Conference Series **225**, 012015 (2010).
- ³⁰ A. Weiss, R. Mayer, M. Jibaly, C. Lei, D. Mehl, and K. G. Lynn, Phys. Rev. Lett. **61**, 2245 (Nov 1988).
- ³¹ W. Werner, H. Tratnik, J. Brenner, and H. Störi, Surface Science **495**, 107 (2001).
- ³² A. Knights and P. Coleman, Surface Science **367**, 238 (1996); M. Farjam and H. B. Shore, Phys. Rev. B **36**, 5089 (Oct 1987).
- ³³ R. Mayer, A. Schwab, and A. Weiss, Phys. Rev. B **42**, 1881 (Aug 1990); E. Soininen, A. Schwab, and K. G. Lynn, *ibid.* **43**, 10051 (May 1991).
- ³⁴ D. Mehl, *Investigation of the surface sensitivity of positron-annihilation- induced auger-electron spectroscopy*, Ph.D. thesis, University of Texas at Arlington (1990).
- ³⁵ "NIST electron inelastic-mean-free-path database," <http://srdata.nist.gov/xps/> (2010).
- ³⁶ R. Mayer, E. Gramsch, and A. Weiss, Phys. Rev. B **40**, 11287 (Dec 1989).
- ³⁷ T. D. Thomas, Phys. Rev. Lett. **52**, 417 (Feb 1984).
- ³⁸ H. A. Fertig, Phys. Rev. Lett. **65**, 2321 (Nov 1990); A. M. Steinberg, *ibid.* **74**, 2405 (Mar 1995); N. L. Chuprikov, Russian Physics journal **49**, 119 (2006); **49**, 314 (2006).
- ³⁹ A. P. Mills, Jr., private communications (2010).
- ⁴⁰ F. J. Himpsel, D. E. Eastman, and E. E. Koch, Phys. Rev. Lett. **44**, 214 (Jan 1980).

- ⁴¹ N. Fazleev, M. Nadesalingam, W. Maddox, S. Mukherjee, K. Rajeshwar, and A. Weiss, *Surface Science* **604**, 32 (2010).
- ⁴² M. Alatalo, B. Barbiellini, M. Hakala, H. Kauppinen, T. Korhonen, M. J. Puska, K. Saarinen, P. Hautojärvi, and R. M. Nieminen, *Phys. Rev. B* **54**, 2397 (Jul 1996).